Inorganic Chemistry
Article
pubs.acs.org/IC

Reactivity of Divalent Germanium Alkoxide Complexes Is in Sharp Contrast to the Heavier Tin and Lead Analogues

Lorenzo Ferro, Peter B. Hitchcock, Martyn P. Coles, and J. Robin Fulton*,†

Department of Chemistry, University of Sussex, Falmer, Brighton BN1 9QJ, United Kingdom

Supporting Information

ABSTRACT: The chemistry of β-diketiminate germanium alkoxide complexes has been examined and shown to be in sharp contrast to its heavier congeners. For instance, (BDI)GeOR (BDI = $[\{N(2,6\text{-}^iPr_2C_6H_3)C(Me)\}_2CH]$, R = ^{i}Pr, ^{s}Bu, ^{t}Bu) does not react with carbon dioxide to form a metal carbonate complex. Addition of aliphatic electrophiles, such as methyl iodide or methyl triflate, results in the net oxidative addition to the germanium, giving cationic tetravalent germanium complexes, [(BDI)Ge(Me)OR][X] (X = I, OTf). An examination of the contrasting reactivities of the alkoxide ligand and the germanium loan pair with Lewis acids yielded the unusual germanium(II)−copper(I) adduct, $\{\mu^2\text{-}Cu_2I_2\}$-$[(BDI)GeO^tBu]_2$. This complex not only displays a rare example of a divalent Ge−Cu bond, but is the first example in which a planar Cu_2I_2 diamond core possesses a three-coordinate copper bound to another metal center.

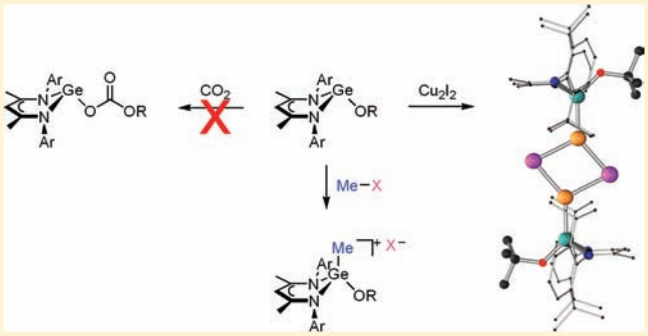

INTRODUCTION

We have recently synthesized a series of β-diketiminate divalent lead- and tin-alkoxide complexes,[1,2] as well as tin-amide complexes,[3] to gauge an understanding of their potential nucleophilicities in comparison to their transition metal counterparts. While these complexes were surprisingly nonreactive with most aliphatic electrophiles, facile, but reversible, insertion of carbon dioxide into the M−O bond of the alkoxides was observed. This reactivity was attributed to the nucleophilic interaction between the alkoxide oxygen atom and the electropositive carbon in carbon dioxide, as well as an electrostatic interaction between the metal center and one of the oxygen atoms of carbon dioxide.[2] It was discovered that the strength of the metal−oxygen bond helped govern both the initial reactivity as well as the reversibility of the carbon dioxide insertion. For instance, the lead alkoxides, with weaker M−O bonds, react much quicker and favor the insertion products more than the isostructural tin systems.

We wished to expand this study to germanium alkoxide complexes. Other β-diketiminate germanium complexes bearing oxygen-based ligands have previously been synthesized, including triflate complexes,[4−6] heterobimetallic complexes in which the metals are bridged by an oxo-ligand,[5,7,8] a germanium hydroxide complex and its complexes with iron and manganese Lewis acids,[9−11] as well as thionocarboxylate and selenocarboxylate derivatives.[12,13] In addition, the germylene ester of formic acid was generated upon treatment of a germanium hydride with carbon dioxide,[14] and germanium phenoxides have also been synthesized.[15] However, outside of coordination chemistry, the reactivity between such complexes with electrophiles has not been examined.

RESULTS AND DISCUSSION

Synthesis. Three β-diketiminate germanium alkoxides complexes, (BDI)GeOR (BDI = $[\{N(2,6\text{-}^iPr_2C_6H_3)C(Me)\}_2CH]^-$), were synthesized by treatment of a THF solution of (BDI)GeCl (**1**) with the appropriate potassium alkoxide, affording germanium alkoxides (BDI)GeO^{i}Pr (**2a**), (BDI)GeO^{s}Bu (**2b**), and (BDI)GeO^{t}Bu (**2c**) (eq 1). The ^{1}H and ^{13}C NMR spectra are similar to the isostructural lead and tin analogues.[1,2] For instance, the ^{1}H NMR spectrum of isopropoxide **2a** exhibits a singlet at δ 4.64 ppm, corresponding to the ligand backbone γ-CH proton. Two sets of apparent septets (δ 3.73 and 3.34 ppm) and four doublets (δ 1.51, 1.49, 1.17, and 1.10 ppm) are also observed, corresponding to the aryl isopropyl groups. This pattern is consistent with a loss of planar symmetry in the BDI-Ge metallocycle, which is due to the trigonal pyramidal geometry of the three-coordinate Ge(II) center.

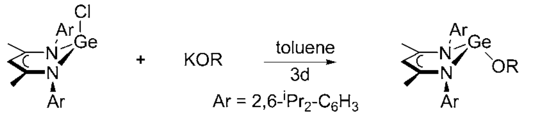

(1)

1

2a, R = ^{i}Pr, 76%
2b, R = ^{s}Bu, 81%
2c, R = ^{t}Bu, 72%

Single crystals of these germanium alkoxide complexes, **2a−2c**, were grown overnight from saturated hexane solutions at −27 °C

Received: August 23, 2011
Published: January 13, 2012

dx.doi.org/10.1021/ic201841m | *Inorg. Chem.* 2012, 51, 1544−1551

(Figure 1). Selected bond lengths and angles are reported in Table 1. Data collection parameters are listed in Table 2. These structures are isomorphous with both the lead and tin analogues, and exhibit a pyramidal geometry around the germanium center due to the presence of a 4s^2 stereochemically active lone pair. An "exo" conformation is observed, with the alkoxide ligand pointing away from the (BDI)-metal core,[3] presumably due to the inability of the bulky alkoxide group to fit in-between the two aromatic rings of the BDI ligand. The Ge−O bond length is longer for the bulkier *tert*-butoxide complex **2c** than the isopropoxide analogue, **2a**.

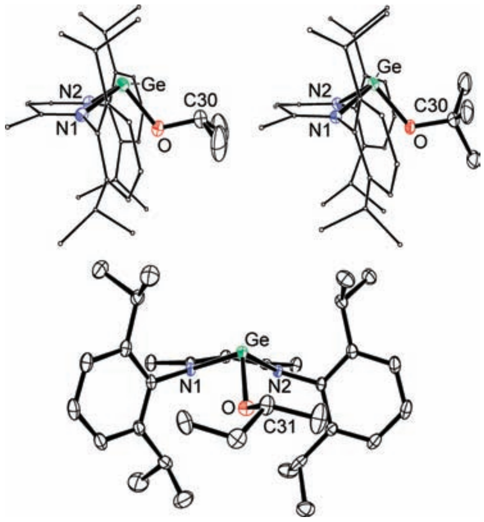

Figure 1. ORTEP diagrams of (BDI)GeO^{i}Pr **2a** (top left), (BDI)GeO^{t}Bu **2c** (top right), and (BDI)GeO^{s}Bu **2b** (bottom middle) with H atoms omitted (for **2a**, **2b**, and **2c**) and BDI aryl group C atoms minimized for clarity (for **2a** and **2c**); ellipsoid probability shown at 30%.

Table 1. Selected Bond Lengths (Å) and Angles (deg) for Compounds 2a, 2b, and 2c

	(BDI)GeO^{i}Pr (**2a**)^a	(BDI) GeO^{s}Bu(**2b**)	(BDI)GeO^{t}Bu (**2c**)
Ge−O	1.821(2)	1.8294(12)	1.8284(3)
Ge−N(1)	2.020(2)	2.0244(14)	2.0222(14)
Ge−N(2)	2.016(2)	2.0234(14)	2.0274(15)
O−C(30)^a	1.432(4)	1.429(4)	1.437(7)
N(1)−Ge−O	96.10(10)	96.70(6)	94.45(6)
N(2)−Ge−O	94.63(10)	96.31(6)	96.00(6)
N(1)−Ge−N(2)	87.74(9)	87.48(5)	87.63(6)
C(30)^a−O−Ge	117.0(2)	116.4(2)	120.9(4)
Ge−NCCCNplane^b	0.853	0.804	0.900
sum of angles around Ge	278.47	280.49	278.08
DP (%)^c	90.6	88.3	91.0

^{a}C(31) for **2b**. ^{b}Distance between Ge and the plane defined by the BDI-backbone (N−C−C−C−N plane). ^{c}Degree of pyramidalization (DP) = [(360 − sum of bond angles)/0.9].[16]

Some general group 14 periodic trends can be observed from these crystal structure data. For instance, the M−O and M−N bond lengths increase with the radius of the metal center, and the N−M−N and N−M−O angles decrease with the larger metal centers, plausibly due to the increase in steric pressure exerted by the more diffuse lone pair. The observed Ge−O bond lengths of germanium alkoxides are shorter than Roesky's aryloxides (BDI)GeOPh (1.860(4) Å) and (BDI)GeOC$_6$F$_5$ (1.95115(14) Å).[15] In contrast, the Ge−N bond lengths of alkoxides **2a**−**2c** are longer, and the N1−Ge−N2 bond angle of our alkoxides is more acute.

Reactivity Studies: Heterocumulenes. In sharp contrast to the lead and tin analogues,[1,2] no reaction is observed between germanium alkoxides **2a** and **2c** and up to 1.5 atm of carbon dioxide, even after heating to 50 °C. This result is consistent with our proposed carbon dioxide insertion mechanism that is dependent upon the M−O bond dissociation energy, which increases going up the group. Similarly, addition of maleic anhydride to germanium alkoxides **2a**−**2c** did not result in a reaction, even at elevated temperatures. Addition of carbon disulfide to **2a**−**2c** resulted in an intractable mixture of products.

Addition of phenyl isocyanate to **2a** did not result in a reaction at room temperature. However, at 50 °C, partial formation of a new compound (**3a**) was observed, with a ratio of **2a** to **3a** of 58:42, as measured by ^{1}H NMR spectroscopy. A doublet at δ 7.01 ppm and two sets of triplets at δ 6.89 and 6.67 ppm were observed in a 2:2:1 ratio, consistent with a new aromatic environment. A singlet was also observed at δ 5.03 ppm and two sets of septets at δ 5.22 and 3.56 ppm in a 1:1:2 ratio, corresponding to the γ-C*H*, the OC*H*Me$_2$, and the Ar−C*H*Me$_2$ protons, respectively. We have tentatively assigned **3a** to be the carbamate species shown in eq 2. The NMR spectral data is similar to that of the isostructural lead carbamate complex. Interestingly, increasing the temperature to 60 °C resulted in a change in ratio of **2a** to **3a** of 64:36. Cooling to room temperature changed the ratio in favor of **3a**; however, this increase was modest as the ratio of **2a** to **3a** was 53:47. Addition of 5 equiv of phenyl isocyanate to **2a** resulted in an intractable mixture of products.

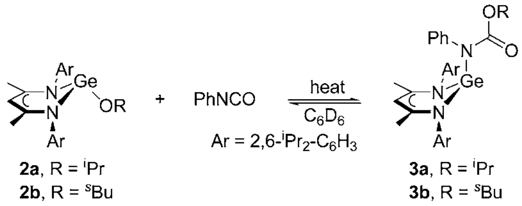

(2)

The germanium *tert*-butoxide complex **2c** does not react with phenyl isocyanate, even at elevated temperatures; whereas the *sec*-butoxide complex **2b** does, presumably forming **3b**. However, similar to the isopropoxide system, an equilibrium is established between **2b** and **3b**, with a 76:24 **2b**:**3b** ratio observed at 60 °C and a 66:34 ratio observed at 50 °C. Cooling to room temperature changed the observed ratio to 59:41.

The low reactivity could be a function of the relatively strong Ge−O bond, requiring a higher activation barrier to react.[2] However, at elevated temperatures, the reactants are favored over the products due to entropic factors playing more of an importance over enthalpic ones. Unfortunately, attempts at qualitatively measuring the equilibrium, as well as gaining further spectroscopic characterization data of **3a** and **3b**, were thwarted by the appearance of an insoluble white precipitate after a few hours at elevated temperatures. In an attempt to fully convert the alkoxides **2a** to **2c** to an isolable product, they were treated with the more reactive PhNCS; however, no reaction was observed at room temperature, and an intractable mixture of products was observed at 50 °C.

Table 2. Crystallographic Data for Compound 2a, 2b, and 2c

	LGeO^{i}Pr (**2a**)	LGeO^{s}Bu (**2b**)^a	LGeO^{t}Bu (**2c**)^b
chemical formula	$C_{32}H_{48}GeN_2O$	$C_{33}H_{50}GeN_2O$	$C_{33}H_{50}GeN_2O$
fw	549.31	563.34	563.34
T (K)	173(2)	173(2)	173(2)
wavelength (Å)	0.710 73	0.710 73	0.710 73
cryst size (mm^3)	0.25 × 0.20 × 0.15	0.21 × 0.16 × 0.12	0.15 × 0.10 × 0.10
cryst system	monoclinic	triclinic	monoclinic
space group	$P2_1/n$ (No.14)	$P\bar{1}$ (No.2)	$P2_1/c$ (No.14)
a (Å)	13.1504(5)	8.5920(1)	13.3507(3)
b (Å)	16.3912(3)	11.7494(3)	16.6088(3)
c (Å)	15.2918(6)	16.6858(4)	16.9602(3)
α (deg)	90	102.907(1)	90
β (deg)	107.328(1)	102.097(2)	121.696 (1)
γ (deg)	90	95.886(1)	90
V (Å^3)	3146.56(18)	1585.59(6)	3199.82(11)
Z	4	2	4
p_c (Mg m^{-3})	1.16	1.18	1.17
abs coeff (mm^{-1})	1.00	0.99	0.983
θ range for data collection (deg)	3.48−26.15	3.46−27.10	3.42−25.86
measured/indep reflns/R(int)	18 604/61 27/0.056	26 337/6947/0.050	44 895/6043/0.061
reflns with $I > 2\sigma(I)$	4769	6133	5144
data/restraints/params	6127/0/337	6947/22/401	6043/133/381
GOF on F^2	1.022	1.023	1.017
final R indices	R1 = 0.048, wR2 = 0.100	R1 = 0.032, wR2 = 0.076	R1 = 0.030, wR2 = 0.069
R indices (all data)	R1 = 0.069, wR2 = 0.111	R1 = 0.040, wR2 = 0.080	R1 = 0.040, wR2 = 0.072
largest diff. peak and hole (e Å^3)	0.54 and −0.82	0.39 and −0.40	0.32 and −0.35

[a] The *sec*-butyl group and one of the isopropyl groups are disordered and were modeled over two positions with loose restraints applied to C−C distances. [b] The ^{t}Bu group is disordered and was modeled over two positions with each restrained to be equal and the carbon atoms of the minor component isotropic.

Reactivity Studies: Aliphatic Electrophiles. The reactivity of germanium alkoxides **2a**−**2c** toward aliphatic electrophiles is also in sharp contrast to the heavier isostructural analogues. For instance, treatment of germanium *tert*-butoxide **2c** with methyl iodide results in the formation of the germanium(IV) cation, [(BDI)Ge(Me)O^{t}Bu)][I] (**4**), as a pale yellow powder in 90% yield (eq 3). The methyl group resonates at δ 1.58 in the ^{1}H NMR spectrum and δ 6.0 ppm in the ^{13}C NMR spectrum. Colorless flakelike crystals suitable for X-ray structural analysis were obtained by leaving the C_6D_6 reaction mixture overnight at room temperature.

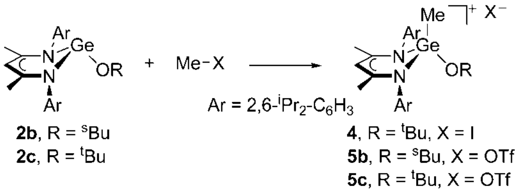

(3)

The ORTEP diagram of **4** is shown in Figure 2. Selected bond lengths and bond angles are listed in Table 3. Data collection parameters are listed in Table 4. The metal center is in a distorted tetrahedral coordination environment. The bond lengths at the metal center are significantly shorter than that of the precursor, *tert*-butoxide **2c**, presumably due to the higher oxidation state of the metal center of **4**. However, the N−Ge−O and N−Ge−N bond angles around germanium are slightly larger. The Ge−C(20) bond length is 1.905(4) Å, which is significantly shorter than both the divalent (BDI)GeMe complex (2.002(4) Å) and the trivalent (BDI)Ge(S)Me complex (2.009(2) Å), possibly due to the cationic nature of **4**.

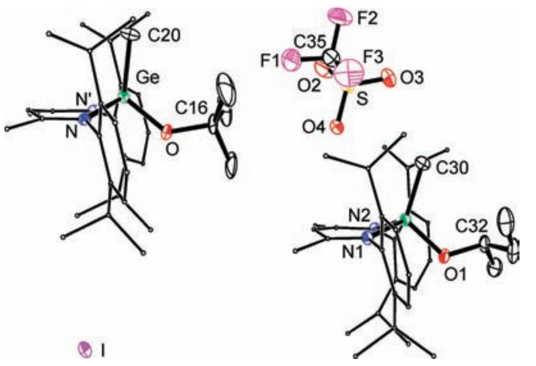

Figure 2. ORTEP diagrams of [(BDI)Ge(Me)O^{t}Bu][I] **4** (left) and [(BDI)Ge(Me)O^{s}Bu][OTf] **5b** (right) with H atoms omitted and BDI aryl groups C atoms minimized for clarity; ellipsoid probability shown at 30%.

Oxidative addition of (BDI)GeMe with methyl iodide has already been reported by Roesky and co-workers; however, the product was not crystallographically characterized.

Similar reactivity was observed by treatment of *sec*-butoxide **2b** and *tert*-butoxide **2c** with the stronger electrophile, MeOTf, resulting in the formation of cationic germanium(IV) complexes [(BDI)Ge(Me)OR][OTf], **5b**, and **5c** (R = sBu, tBu). The ^{1}H NMR spectroscopic analysis shows the terminal methyl group resonating at δ 1.44 (**5b**) and 1.62 (**5c**) ppm. The corresponding ^{13}C NMR spectroscopic resonances are observed at δ 6.1 (**5b**) and 6.0 (**5c**) ppm. The ^{19}F NMR spectrum shows a singlet at δ −78.19 (**5b**) and −78.31 (**5c**) ppm, corresponding to the anionic triflate group. Colorless crystals of **5b** suitable for an X-ray diffraction study were obtained from a saturated tetrahydrofuran solution of **5b** after two weeks at −27 °C (Figure 2). Similar to **4**, the metal center of **5b** possesses a distorted tetrahedral coordination geometry. The bond lengths and angles are also similar, with the exception of the longer Ge−O bond and the more acute O−Ge−C and Ge−O−C bond angles. These latter differences are attributed to the different alkoxide groups on the germanium center.

Table 3. Selected Bond Lengths (Å) and Angles (deg) for Compounds 4 and 5b

	[LGe(Me)(O^{t}Bu)][I] (**4**)	[LGe(Me)(O^{s}Bu)][OTf] (**5b**)
Ge−O(1)	1.723(3)	1.7422(15)
Ge−N(1)[a]	1.877(3)	1.8808(17)
Ge−N(2)[a]		1.8678(17)
Ge−C(20) (30)	1.904(5)	1.910(2)
O−C(16) (32)	1.479(7)	1.469(4)
N(1)−Ge−O	105.95(10)	107.11(7)
N(2)−Ge−O		106.90(8)
N(1)−Ge−N(2)	98.62(15)	98.40(7)
O−Ge−C(20)	122.2(2)	114.56(9)
N(1)−Ge−C(20)	110.74(13)	112.43(9)
N(2)−Ge−C(20)		115.95(9)
Ge−O−C(16) (32)	131.9(4)	121.2(2)
Ge−C_3N_2 plane[b]	0.607	0.503

[a] N and N′ for **4**. [b] Distance between Ge and the plane defined by the BDI-backbone (N−C−C−C−N plane).

The oxidative addition chemistry of the alkoxides was further examined by treatment of *tert*-butoxide **2c** with molecular iodine, which results in the formation of the cationic complex [(BDI)Ge(I)O^{t}Bu][I_3], **6** (eq 4). This complex is presumably

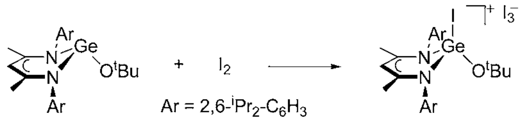

2c **6** (4)

formed by the reaction of the iodide counterion of the transient species, [(BDI)Ge(I)O^{t}Bu][I] with a further equivalent of iodine, to give the more stabilizing counteranion, $[I_3]^-$. Compound **6** can be obtained in 92% yield as a dark orange powder and was characterized by multinuclear NMR spectroscopy, IR spectroscopy, as well as combustion analysis. The very low field singlet resonance of the methinic γ-C*H* proton in the ^{1}H NMR spectrum (δ 6.47 ppm) is reminiscent of the cationic hypervalent germanium BDI complexes **4** (δ 6.10 ppm), **5b** (δ 5.99 ppm), and **5c** (δ 6.04 ppm). Deep orange crystals suitable for an X-ray diffraction study were grown from a tetrahydrofuran/fluorobenzene mixture. Unfortunately, the X-ray diffraction study of complex **6** did not give high quality data; however, the connectivity was confirmed.

Reactivity Studies: Lewis Acids. In order to gauge the Lewis base behavior of the germanium alkoxides, **2a**−**2c**, a tetrahydrofuran solution of *tert*-butoxide **2c** was treated with copper(I) iodide, to afford the germanium(II)−copper(I)

Table 4. Crystallographic Data for Compound 4, 5b, and 7

	[LGe(Me)(O^{t}Bu)][I] (**4**)[a]	[LGe(Me)(O^{s}Bu)][OTf] (**5b**)···1.5THF[b]	[{(BDI)GeO^{t}Bu}·CuI]$_2$ · 3 C_7H_8 (**7**)[c]
chemical formula	$C_{34}H_{53}GeIN_2O$	$C_{82}H_{130}F_6Ge_2N_4O_{11}S_2$	$C_{66}H_{100}Cu_2Ge_2I_2N_4O_2$, $3(C_7H_8)$
fw	705.27	1671.26	1784.02
T (K)	173(2)	173(2)	173(2)
wavelength (Å)	0.710 73	0.710 73	0.710 73
cryst size (mm^3)	0.40 × 0.30 × 0.25	0.34 × 0.25 × 0.18	0.14 × 0.06 × 0.04
cryst syst	orthorhombic	triclinic	monoclinic
space group	*Pnma* (No.62)	$P\bar{1}$ (No.2)	*C*2/*m* (No.12)
a (Å)	21.2060(4)	12.7878(4)	15.7342(5)
b (Å)	18.5239(7)	13.0690(3)	16.4339(7)
c (Å)	8.9409(3)	13.4060(5)	16.7541(7)
α (deg)	90	86.982(2)	90
β (deg)	90	83.786(2)	102.306(2)
γ (deg)	90	83.477(2)	90
V (Å^3)	3512.15(19)	2211.03(12)	4232.6(3)
Z	4	1	2
p_c (Mg m^{-3})	1.33	1.26	1.40
abs coeff (mm^{-1})	1.78	0.796	1.98
θ range for data collection (deg)	3.67−26.04	3.43−27.48	3.51−27.11
measured/indep reflns/*R*(int)	15 322/3538/0.065	36 161/10 017/0.048	22 306/4843/0.089
reflns with $I > 2\sigma(I)$	2763	8565	3319
data/restraints/params	3538/24/208	10 017/84/514	4843/67/239
GOF on F^2	1.016	1.041	1.002
final *R* indices	R1 = 0.039, wR2 = 0.086	R1 = 0.043, wR2 = 0.109	R1 = 0.052, wR2 = 0.091
R indices (all data)	R1 = 0.057, wR2 = 0.095	R1 = 0.055, wR2 = 0.117	R1 = 0.095, wR2 = 0.103
largest diff peak and hole (e Å^3)	0.53 and −0.91	0.65 and −0.39	1.01 and −0.59

[a] The Bu group was included as disordered across the mirror plane and with restraints on the C−C(Me) and C(Me)···C(Me) distances. [b] The *sec*-butoxy group was disordered over two positions. It was not possible to distinguish between the carbon and oxygen atom positions on either THF solvate; they were therefore refined with carbon at 80% occupancy and oxygen at 20% occupancy for each position. The THF molecule on the inversion center was also modeled with all atoms left isotropic. [c] The ^{t}Bu group disordered about a mirror plane and was refined with carbon atoms left isotropic. One of the ^{i}Pr groups is disordered over two positions; the toluene solvates are disordered about special positions.

adduct $\{\mu^1\text{-}Cu_2I_2\}[(BDI)GeO^tBu]_2$ **7** in 61% yield (eq 5). The ^{1}H NMR spectrum reveals a broad resonance for the isopropyl methine protons (δ 3.46 ppm); unfortunately, sharper singles were not observed upon heating to 40 °C and cooling to −60 °C of the d_8-THF NMR sample.

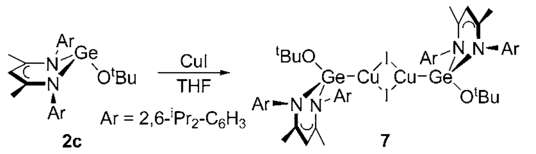

(5)

Complex **7** crystallizes from a saturated toluene solution after a month and a half at −27 °C (Figure 3). Selected bond lengths and angles are listed in Table 5. Data collection parameters are given in Table 4. The molecule lies on a crystallographical mirror plane and possesses an inversion center. As a result, there is a planar arrangement of the germanium, oxygen, carbon (C16), copper, and iodide atoms (Figure 4). The bond lengths around the germanium center are in between that of the parent alkoxide **2c** and cationic complex **4**, indicating a slight increase of positive charge around the germanium center due to electron donation into the empty s orbital of Cu(I).

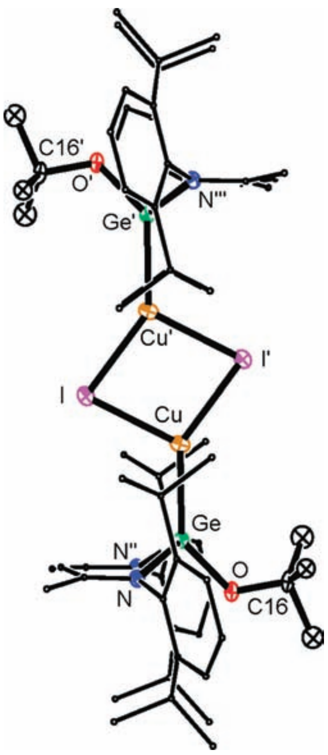

Figure 3. ORTEP diagram of $\{\mu^1\text{-}Cu_2I_2\}\{(BDI)GeO^tBu\}_2$ **7** with H atoms omitted and BDI aryl group C atoms minimized for clarity; ellipsoid probability shown at 30%.

Table 5. Selected Bond Lengths (Å) and Angles (deg) for Compound 7

Ge−O	1.781(4)	N−Ge−N″	91.3(2)
Ge−N	1.964(3)	N−Ge−O	96.87(14)
Ge−Cu	2.3341(10)	N−Ge−Cu	113.29(10)
Cu−I	2.6382(9)	O−Ge−Cu	135.71(14)
Cu−I′	2.5791(9)	C16−O−Ge	125.3(4)
O−C16	1.447(7)	Ge−Cu−I	116.99(4)
Cu···Cu′	3.297(2)	Ge−Cu−I′	141.37(4)
I···I	4.0443(9)	Cu−I−Cu′	78.37(3)
		I−Cu−I′	101.63(3)
Ge−C_3N_2 plane	0.865		

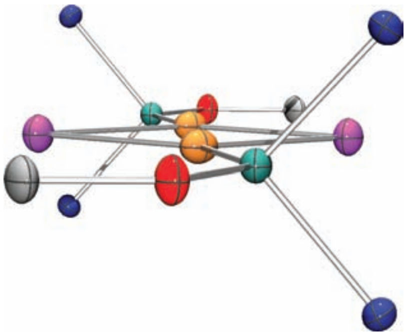

Figure 4. POV-Ray diagram of the core of **7**. Only C16, Cu, Ge, I, N, and O atoms are shown for clarity. Color code: C16, gray; Cu, copper, Ge, turquoise; I, purple; N, blue; O, red.

Only a few other complexes possessing Cu−Ge bonds are known. The Ge−Cu distance of **7** (2.3341(10) Å) is longer than that observed by Mochida and co-workers for their series of copper−germylene complexes, [(^{i}Pr-nacnac)Cu−Ge(X)(^{i}Pr-nacnac)] (Ge−Cu bond length: X = Cl, 2.3109(4) Å; X = H, 2.2980(8), X = Me 2.3165(3), ^{i}Pr-nacnacH = 2-(isopropylamino)-4-(isopropylimino)-2-pentene).[17] It is also longer than that reported by Tolman and co-workers in their [(BDI)CuGeY] complexes (Ge−Cu bond length: Y = $[(NMes)_2(CH)_2]$, 2.2138(4) Å; Y = $[N(SiMe_3)_2)]_2$, 2.2492(4) Å).[18] However, our Ge−Cu bond length is shorter than reported by Leung and co-workers. In their system, four germanium complexes, $[Ge\{N(SiMe_3)C(Ph)C(SiMe_3)(C_5H_4N\text{-}2)\}Cl]$, are coordinated to each copper vertex of a Cu_4I_4 cubane cluster.[19]

The Cu_2I_2 ring of complex **7** has a rhomboidal shape. The Cu−I bond lengths of 2.5791(9) and 2.6382(9) Å are similar to other rhomboidal Cu_2I_2 complexes, with a standard bond length of between 2.50 and 2.57 Å for symmetric systems,[20−23] or 2.54 and 2.64 Å for asymmetric systems.[20,24] This latter type of bonding can arise from the weak interaction of two LCuI monomers.[25] The Cu−I−Cu′ and I−Cu−I′ angles are 78.37(3)° and 101.63°, respectively. The Cu···Cu′ distance in is 3.297(2) Å, too far for any Cu−Cu bonding interaction to occur.[21,25,26]

Compound **7** is the second example in which a Cu_2X_2 unit (X = Cl, Br, I) possesses three-coordinate copper centers bound to another metal.[27] The other known example is $[Cp_2ReHCuI]_2$;[27] however, instead of the standard planar Cu_2I_2 arrangement, the Cu_2I_2 unit is folded, resulting in a short Cu···Cu′ distance of 2.552(4) Å, indicative of a formal Cu−Cu bond.[21,25,26] Other examples the Cu_2X_2 unit with a M−Cu bond, but a higher coordination number at copper, include Mo(W)−S clusters,[28] Mo−Sb clusters,[29] an Fe−(CO) cluster,[30] vinylidene- and aminocarbyne-bridged heterobimetallic complexes,[31,32] a centrosymmetric $[Cu_4I_8]^{4-}$ complex,[33] and a Cu_2X_2 unit coordinated at each copper by two $SbPh_3$ ligands.[34]

■ CONCLUSIONS

A series of germylene alkoxide complexes have been synthesized. In contrast to the isostructural tin and lead systems, germanium(II) β-dikeiminate alkoxide complexes do not activate carbon dioxide, further supporting the dependence on the metal−oxygen bond dissociation energy being key for such a reaction to occur; that is, reactivity toward insertion increases with decreasing BDE. Alkoxides **2a**−**2c** also present a different reactivity toward aliphatic electrophiles, resulting in the formation of cationic oxidative addition products. This reactivity is a result of the germanium lone pair being more energetically accessible than the oxygen's one, as well as divalent germanium's propensity to be oxidized to its tetravalent state. The pronounced Lewis base behavior of the germanium center was also confirmed by the addition of copper(I) iodide, which results in the formation of a Ge(II)−Cu(I) adduct, possessing an unusual planar Cu$_2$I$_2$ ring bridging two metal centers.

■ EXPERIMENTAL SECTION

General. All manipulations were carried out in an atmosphere of dry nitrogen using standard Schlenk techniques or in an inert-atmosphere glovebox. Solvents were dried from the appropriate drying agent, distilled, degassed, and stored over 4 Å sieves. (BDI)H and (BDI)GeCl were prepared according to literature procedures,[35] although a slightly modified procedure was used in the synthesis of GeCl$_2$(diox). Potassium alkoxide salts were prepared by the slow addition of the relevant alcohol (dried and distilled) to a suspension of potassium hydride. Methyl iodide and methyl trifluoromethanesulfonate were freshly dried and distilled before use. Carbon dioxide was used as received (Union Carbide, 99.999%). ^{1}H and ^{13}C NMR spectra were recorded on a Varian 400 MHz or Varian 500 MHz spectrometer. ^{1}H and ^{13}C NMR spectroscopic chemical shifts are given relative to residual solvent peaks, and the ^{19}F chemical shifts were externally referenced to CFCl$_3$. The data for the X-ray structures were collected at 173 K on a Nonius Kappa CCD diffractometer, k(Mo Kα) = 0.710 73 Å and refined using the *SHELXL-97* software package.[36]

[GeCl$_2$·(dioxane)]. [37] GeCl$_4$ (20 mL, 87.7 mmol) and 1,4-dioxane (15 mL) were dissolved in a 1:1 hexane:Et$_2$O mixture (100 mL). To this mixture was added ^{n}Bu$_3$SnH (25 mL, 92.9 mmol). After stirring at room temperature for 30 min, a white precipitate appeared. This was filtered off, washed with cold hexane, and identified as the pure GeCl$_2$(diox) (2 g). The mother liquor was left at room temperature for 2 days, affording white crystals of GeCl$_2$(diox) (17.0 g) upon standing, for a total combined yield of 84%. Note that repeated experiments on a smaller scale resulted in a considerably lower yield (10−18%).

[CH{(CH$_3$)CN-2,6-^{i}Pr$_2$C$_6$H$_3$}$_2$GeO^{i}Pr] (2a). A suspension of KO^{i}Pr (94 mg, 0.95 mmol) in THF (5 mL) was added to a solution of (BDI)GeCl (0.50 g, 0.95 mmol) in THF (5 mL) at room temperature, and the reaction mixture was stirred for 3 days. The solvent was removed under vacuum, the orange crude product was extracted with toluene, and the solution was filtered through celite. Removal of the volatiles and recrystallization from hexane overnight at −27 °C afforded orange crystals of (BDI)GeO^{i}Pr **2a** (0.38 g, 72%). ^{1}H NMR (400 MHz, C$_6$D$_6$, 303 K): δ 7.17−7.02 (m, 6H, Ar-*H*), 4.64 (s, 1H, γ-C*H*), 3.73 (m, 3H, C*H*Me$_2$ + OC*H*Me$_2$), 3.34 (m, 2H, C*H*Me$_2$), 1.51 (s, 6H, NC*Me*), 1.49 (d, J = 6.8 Hz, 6H, CH*Me*), 1.17 (d, J = 6.9 Hz, 6H, CH*Me*), 1.10 (d, J = 6.8 Hz, 6H, CH*Me*), 0.57 (d, J = 6.1 Hz, 6H, OCH*Me*). ^{13}C{^{1}H} NMR (400 MHz, CDCl$_3$): δ 163.29 (NCMe), 145.04 (*ipso-C*), 139.20 (*Ar*−*C*), 126.45 (*Ar*−*C*), 124.66 (*Ar*−*C*), 123.97 (*Ar*−*C*), 94.99 (γ -CH), 64.93 (OCHMe$_2$), 28.40 (NC*Me*), 27.97 (NC*Me*), 26.31 (CHMe),24.45 (CHMe), 24.24 (CH*Me*), 22.70 (CH*Me*), 22.31 (CH*Me*), 20.37 (CH*Me*). IR (Nujol, υ/cm^{-1}): 1561, 1521, 1321, 1260, 1174, 1019, 964, 795. Anal. Calcd for C$_{32}$H$_{48}$GeN$_2$O: C, 69.96; H, 8.81; N, 5.10. Found: C, 69.84; H, 8.72; N, 4.92.

[CH{(CH$_3$)CN-2,6-^{i}Pr$_2$C$_6$H$_3$}$_2$GeO^{s}Bu] (2b). Orange crystals suitable for an X-ray crystallographic study of (BDI)GeO^{s}Bu **2b** can be obtained in a similar way to **2a** in 81% yield. ^{1}H NMR (400 MHz, C$_6$D$_6$, 303 K): δ 7.20−7.02 (m, 6H, Ar-*H*), 4.66 (s, 1H, γ-C*H*), 3.84−3.68 (m, 2H, C*H*Me$_2$), 3.55−3.43 (m, 1H, OC*H*(Me)Et), 3.37 (m, 2H, C*H*Me$_2$), 1.51 (s, 3H, NC*Me*), 1.50 (s, 3H, NC*Me*), 1.48 (d, J = 7.4 Hz, 6H, CH*Me*), 1.34 (d, J = 6.3 Hz, 6H, CH*Me*), 1.33 (d, J = 6.4 Hz, 6H, CH*Me*), 1.19 (d, J = 6.9 Hz, 7H), 1.08−0.94 (m, 2H, OC(Me)C*H$_2$*Me), 0.45 (d, J = 6.2 Hz, 3H, OCH(*Me*)Et), 0.26 (t, J = 7.4, 3H, OCH(Me)CH$_2$*Me*). ^{13}C{^{1}H } NMR (400 MHz, C$_6$D$_6$): δ 163.24 (NCMe), 144.17 (*ipso-C*), 137.03 (*Ar*−*C*), 126.59 (*Ar*−*C*), 124.13 (*Ar -C*), 124.02 (*Ar*−*C*), 95.20 (γ-CH), 70.68 (OC(Me)Et), 33.37 (OCH(Me)CH$_2$Me), 28.37 (NC*Me*), 28.25 (NC*Me*), 26.24 (CHMe), 24.41 (CHMe), 23.02 (CH*Me*), 22.34 (CH*Me*), 21.77 (CH*Me*), 20.38 (OCH(*Me*)Et), 10.02 (OCH(Me)CH$_2$*Me*). IR (Nujol, υ/cm^{-1}): 1557, 1522, 1320, 1175, 1018, 918, 795. Anal. Calcd for C$_{33}$H$_{50}$GeN$_2$O: C, 70.35; H, 8.95; N, 4.97. Found: C, 70.46; H, 9.01; N 4.87.

[CH{(CH$_3$)CN-2,6-^{i}Pr$_2$C$_6$H$_3$}$_2$GeO^{t}Bu] (2c). Orange crystals suitable for an X-ray crystallographic study of (BDI)GeO^{t}Bu **2c** can be obtained in a similar way to **2a** in 76% yield. ^{1}H NMR (400 MHz, C$_6$D$_6$, 303 K): δ 7.25 − 6.96 (m, 6H, Ar−*H*), 4.61 (s, 1H, γ-C*H*), 3.82 (m, 2H, C*H*Me$_2$), 3.34 (sept, J = 6.8 Hz, 2H, C*H*Me$_2$), 1.51 (s, 6H, NC*Me*), 1.50 (d, J = 7.2 Hz, 6H, CH*Me*), 1.33 (d, J = 6.8 Hz, 6H, CH*Me*), 1.16 (d, J = 6.9 Hz, 6H, CH*Me*), 1.10 (d, J = 6.8 Hz, 6H, CH*Me*), 0.78 (s, 9H, OC*Me$_3$*). ^{13}C{^{1}H} NMR (400 MHz, CDCl$_3$): δ 163.61 (NCMe), 145.16 (*ipso-C*), 139.66 (*Ar*−*C*), 126.45 (Ar*p*−*C*), 124.66 (*Ar*−*C*), 123.71 (*Ar*−*C*), 96.03 (γ-CH), 70.00 (OCMe$_3$), 33.21 (OC*Me$_3$*), 28.47 (NC*Me*), 27.08 (NC*Me*), 26.46 (CHMe$_2$), 25.82 (CHMe$_2$), 24.86 (CH*Me*), 22.44 (CH*Me*). IR (Nujol, υ/cm^{-1}): 1553, 1520, 1322, 1260, 1175, 1100, 1020, 935, 795. Anal. Calcd for C$_{33}$H$_{50}$GeN$_2$O: C, 70.35; H, 8.95; N, 4.97. Found: C, 70.49; H, 9.05; N, 4.90.

[CH{(CH$_3$)CN-2,6-^{i}Pr$_2$C$_6$H$_3$}$_2$Ge(Me)O^{t}Bu]I (4). MeI (7.8 μL, 0.12 mmol) was added to a stirring toluene solution (5 mL) of (BDI)GeO^{t}Bu **2c** (70 mg, 0.12 mmol). After 1 h, the solution turned a pale yellow, and a pale yellow precipitate was formed. The volatiles were removed, and the solid was washed with cold pentane affording a pale yellow powder of [(BDI)Ge(Me)O^{t}Bu]I **4** in 90% yield (78 mg). Colorless crystals suitable for an X-ray crystallographic study can be obtained by performing the reaction without stirring and leaving the reaction mixture overnight at room temperature. ^{1}H NMR (500 MHz, CD$_2$Cl$_2$): δ 7.51 (t, J = 7.8, 2H, Ar−*H*), 7.38 (d, J = 7.8, 4H, Ar−*H*), 6.10 (s, 1H, γ-C*H*), 3.14 (m, 2H, C*H*Me$_2$), 2.92 (m, 2H, C*H*Me$_2$), 2.18 (s, 6H, NC*Me*), 1.58 (s, 3H, Ge*Me*), 1.43 (d, J = 6.8 Hz, 6H, CH*Me$_2$*), 1.36 (d, J = 6.7 Hz, 6H, CH*Me$_2$*), 1.34 (d, J = 6.6 Hz, 6H, CH*Me$_2$*), 1.14 (d, J = 6.8 Hz, 6H, CH*Me$_2$*), 0.74 (s, 9H, OC*Me*). ^{13}C{^{1}H } NMR (400 MHz, CD$_2$Cl$_2$): δ 173.60 (NCMe), 145.31 (*ipso-C*), 130.28 (*Ar*−*C*), 125.67 (*Ar*−*C*), 125.39 (*Ar*−*C*), 100.75 (γ-CH), 75.58 (OCMe$_3$), 31.39 (OC*Me$_3$*), 29.14 (NC*Me*), 28.01 (NC*Me*), 25.29 (CHMe$_2$), 24.99 (CHMe$_2$), 24.51 (CH*Me*), 23.61 (CH*Me*), 6.0 (Ge*Me*). IR (Nujol, υ/cm^{-1}): 3059, 1624, 1553, 1363, 1253, 1176, 1101, 935, 799, 785, 758. Anal. Calcd for C$_{34}$H$_{53}$GeIN$_2$O: C, 57.90; H, 7.57; N, 3.97. Found: C, 57.84; H, 7.55; N, 3.91.

[CH{(CH$_3$)CN-2,6-^{i}Pr$_2$C$_6$H$_3$}$_2$Ge(Me)O^{s}Bu]OTf (5b). (BDI)-GeO^{s}Bu **2b** (230 mg, 0.41 mmol) was dissolved in pentane (5 mL) and treated with methyl triflate (45 μL, 0.41 mmol). The reaction mixture was stirred for 1 h, after which a pale yellow precipitate was formed. The solution was decanted and the residue washed with pentane. Storage of a saturated THF solution at −27 °C for 2 weeks yielded colorless crystals of [(BDI)Ge(Me)O^{t}Bu]OTf **5b** (229 mg, 77%), suitable for X-ray crystallography. ^{1}H NMR (399 MHz, CDCl$_3$): δ 7.29 (m, 6H, Ar−*H*), 5.99 (s, 1H, γ-C*H*), 3.28 (m, 1H, OC*H*(Me)Et), 3.12 (m, 2H, C*H*Me$_2$), 3.03 (m, 2H, C*H*Me$_2$), 2.13 (s, 3H, NC*Me*), 2.11 (s, 3H, NC*Me*), 1.44 (s, 3H, Ge*Me*), 1.29 (d, 6H, J = 5.8, CH*Me*), 1.27 (m, 2H, OC(Me)C*H$_2$*Me), 1.14 (d, 6H, J = 6.9 Hz, CH*Me*), 1.06 (d, 6H, J = 6.8 Hz, CH*Me*), 0.81 (d, 6H, J = 6.8 Hz, CH*Me*), 0.32 (d, 3H, J = 6.0 Hz, OCH(*Me*)Et), 0.15 (t, 3H, J = 7.5 Hz, OCH(Me)CH$_2$*Me*). ^{13}C{^{1}H } NMR (399 MHz, CDCl$_3$): δ 172.7 (NCMe), 145.2 (*ipso-C*), 130.0 (*Ar*−*C*), 125.1 (*Ar*−*C*), 123.4 (*Ar*−*C*), 102.1 (γ-CH), 74.8 (OCH(Me)Et), 28.7 (NC*Me*), 27.4 (CHMe), 24.8 (CH*Me*), 24.4 (OCH(Me)CH$_2$Me), 23.8 (CH*Me*), 22.4 (OCH(*Me*)-Et), 9.18 (O(Me)CH$_2$*Me*), 0.0 (Ge*Me*). ^{19}F NMR (400 MHz, CDCl$_3$): δ −78.31. IR (Nujol, υ/cm^{-1}): 1549, 1378 (s), 1370 (s), 1323, 1269 (s), 1235, 1150, 1110, 1032 (s), 955, 810, 762, 637. Anal.

Calcd for $C_{35}H_{35}F_3N_2O_4GeS$: C, 57.78; H, 7.34; N, 3.85. Found: C, 57.83; H, 7.40; N, 3.76.

[CH{(CH$_3$)CN-2,6-^{i}Pr$_2$C$_6$H$_3$}$_2$Ge(Me)O^{t}Bu]OTf (5c). [(BDI)Ge(Me)O^{s}Bu]OTf **5c** can be obtained as a pale yellow powder in 72% yield using a similar methodology for the generation of **5b**. ^{1}H NMR (399 MHz, CDCl$_3$): δ 7.36 (m, 6H, Ar−*H*), 6.04 (s, 1H, γ-C*H*), 3.16 (m, 2H, C*H*Me$_2$), 3.06 (sept, 2H, *J* = 6.6, C*H*Me$_2$), 2.15 (s, 6H, NC*Me*), 1.62 (s, 3H, Ge*Me*), 1.40 (d, 6H, *J* = 6.8, CH*Me*), 1.32 (d, 6H, *J* = 6.7, CH*Me*), 1.31 (d, 6H, *J* = 6.5, CH*Me*), 1.11 (d, 6H, *J* = 6.9, CH*Me*), 0.71 (s, 9H, OC*Me*$_3$). ^{13}C{^{1}H } NMR (399 MHz, CDCl$_3$): δ 173.6 (NCMe), 146.0 (*ipso*-*C*), 130.0 (*Ar*−*C*), 125.6(*Ar*−*C*), 124.9 (*Ar*−*C*), 120.9 (SO$_3$CF$_3$), 101.7 (γ -CH), 88.5 (OCMe$_3$), 31.56 (OC*Me*$_3$), 29.07 (NC*Me*), 27.7 (CHMe$_2$), 25.5 (CHMe$_2$), 25.1 (CH*Me*), 24.7 (CH*Me*), 24.0 (CH*Me*), 23.8 (CH*Me*), 6.1 (Ge*Me*). ^{19}F NMR (400 MHz, CDCl$_3$): δ −78.19. IR (Nujol, υ/cm^{-1}): 1544, 1377 (s), 1366 (s), 1318, 1266 (s), 1223, 1149, 1106, 1030 (s), 947, 894 (w), 808, 752, 637. Anal. Calcd for $C_{35}H_{35}F_3N_2O_4GeS$: C, 57.78; H, 7.34; N, 3.85. Found: C, 57.99; H, 7.48; N, 3.73.

[CH{(CH$_3$)CN-2,6-^{i}Pr$_2$C$_6$H$_3$}$_2$Ge(I)O^{t}Bu]I$_3$ (6). Iodine (46 mg, 0.24 mmol) was added to a toluene solution (5 mL) of (BDI)GeO^{t}Bu **2c** (52 mg, 0.09 mmol). The reaction mixture was stirred overnight producing a pale precipitate. The solution was decanted, and the precipitate was washed several times with pentane, affording [(BDI)Ge(I)O^{t}Bu]I$_3$ **6**, a dark orange powder in 92% yield (89 mg). Dark red crystals were obtained by storing a THF/C$_6$H$_5$F solution of **6** at −27 °C for one week. ^{1}H NMR (400 MHz, CDCl$_3$): δ 7.50 (t, *J* = 7.8, 2H, Ar−*H*), 7.40 (d, *J* = 7.8, 2H, Ar−*H*), 7.34 (d, *J* = 7.8, 2H, Ar−*H*), 6.47 (s, 1H, γ-C*H*), 3.24 (m, 2H, C*H*Me$_2$), 3.11 (m, 2H, C*H*Me$_2$), 2.33 (s, 6H, NC*Me*), 1.43 (d, *J* = 6.8 Hz, 6H, CH*Me*$_2$), 1.40 (d, *J* = 7.5 Hz, 6H, CH*Me*$_2$), 1.38 (d, *J* = 7.1 Hz, 6H, CH*Me*$_2$), 1.11 (d, *J* = 6.8 Hz, 6H, CH*Me*$_2$), 0.90 (s, 9H, OC*Me*$_3$). ^{13}C{^{1}H } NMR (400 MHz, CDCl$_3$): δ 174.75 (NCMe), 146.68 (*ipso*-*C*), 130.80 (*Ar*−*C*), 126.53 (*Ar*−*C*), 125.04 (*Ar*−*C*), 102.83 (γ-CH), 82.80 (OCMe$_3$), 31.57 (OC*Me*$_3$), 29.57 (NC*Me*), 28.94 (NC*Me*), 28.00 (CHMe$_2$), 25.54 (CHMe$_2$), 25.01 (CH*Me*), 23.56 (CH*Me*). IR (Nujol, υ/cm^{-1}): 1541, 1519, 1317, 1251, 1158, 1024, 933, 810. Anal. Calcd: C, 37.01 ; H, 4.71; N, 2.62. Found: C, 36.86; H, 4.62; N, 2.49.

{μ-(CuI)$_2$}[CH{(CH$_3$)CN-2,6-^{i}Pr$_2$C$_6$H$_3$}$_2$GeO^{t}Bu]$_2$ (7). THF (5 mL) was added to a stirring solid mixture of CuI (18 mg, 0.09 mmol) and (BDI)GeO^{t}Bu **15c** (52 mg, 0.09 mmol). After stirring for 3 days, volatiles were removed under vacuum and the resulting precipitate was extracted with toluene and filtered through celite. Removal of the volatiles and washing with cold pentane afforded (BDI)Ge(O^{t}Bu)CuI **7** as a bright yellow powder in 61% yield (43 mg). Storage at −27 °C for one month of a concentrated toluene solution of **7** afforded pale yellow crystals suitable for an X-ray crystallographic study. ^{1}H NMR (400 MHz, d_8-THF): δ 7.21 (m, 12H, Ar−*H*), 5.01 (s, 2H, γ-C*H*), 3.56 (br, 8H, C*H*Me$_2$), 1.76 (s, 12H, NC*Me*), 1.44 (d, *J* = 5.9 Hz, 12H, CH*Me*$_2$), 1.39 (d, *J* = 6.8 Hz, 12H, CH*Me*$_2$), 1.27 (d, *J* = 6.7 Hz, 12H, CH*Me*$_2$), 1.13 (d, *J* = 6.8 Hz, 12H, CH*Me*$_2$), 0.67 (s, 18H, OC*Me*$_3$). ^{13}C{^{1}H} NMR (400 MHz, d_8-THF): δ 165.74 (NCMe), 145.11 (*ipso*-*C*), 135.59 (*Ar*−*C*), 123.58 (*Ar*−*C*), 122.72 (*Ar*−*C*), 99.03 (γ-CH), 67.93 (OCMe$_3$), 32.87 (OC*Me*$_3$), 28.61 (NC*Me*), 28.20 (NC*Me*), 24.81 (CHMe$_2$), 23.85 (CHMe$_2$), 22.45 (CH*Me*), 22.21 (CH*Me*). IR (Nujol, υ/cm^{-1}): 2321, 1523, 1261, 1097, 1020, 936, 802. Repeated attempts of obtaining elemental analysis for compound **7** were unsuccessful. The ^{1}H NMR spectrum of the crystals of **7** is consistent with that of the product formed upon initial reaction.

■ ASSOCIATED CONTENT

Ⓢ Supporting Information

Crystallographic data for **2a**, **2b**, **2c**, **4**, **5b**, and **7** (CIF). NMR spectrum of **7**. This material is available free of charge via the Internet at http://pubs.acs.org.

■ AUTHOR INFORMATION

Corresponding Author

*E-mail: j.robin.fulton@vuw.ac.nz.

Present Address

[†] School of Chemical and Physical Sciences, Victoria University of Wellington, PO Box 600, Wellington, New Zealand.

■ ACKNOWLEDGMENTS

The authors are grateful for the financial support from the EPSRC (L.F., Grant EP/E032575/1).

■ REFERENCES

(1) Tam, E. C. Y.; Johnstone, N. C.; Ferro, L.; Hitchcock, P. B.; Fulton, J. R. *Inorg. Chem.* **2009**, *48*, 8971−8976.

(2) Ferro, L.; Hitchcock, P. B.; Coles, M. P.; Cox, H.; Fulton, J. R. *Inorg. Chem.* **2011**, *50*, 1879−1888.

(3) Harris, L. A. M.; Coles, M. P.; Fulton, J. R. *Inorg. Chim. Acta* **2011**, *369*, 97−102.

(4) Yao, S. L.; Brym, M.; Merz, K.; Driess, M. *Organometallics* **2008**, *27*, 3601−3607.

(5) Saur, I.; Alonso, S. G.; Gornitzka, H.; Lemierre, V.; Chrostowska, A.; Barrau, J. *Organometallics* **2005**, *24*, 2988−2996.

(6) Driess, M.; Yao, S. L.; Brym, M.; van Wullen, C. *Angew. Chem., Int. Ed.* **2006**, *45*, 4349−4352.

(7) Yang, Y.; Roesky, H. W.; Jones, P. G.; So, C. W.; Zhang, Z. S.; Herbst-Irmer, R.; Ye, H. Q. *Inorg. Chem.* **2007**, *46*, 10860−10863.

(8) Doyle, D. J.; Hitchcock, P. B.; Lappert, M. F.; Li, G. *J. Organomet. Chem.* **2009**, *694*, 2611−2617.

(9) Pineda, L. W.; Jancik, V.; Roesky, H. W.; Necuali, D.; Neculai, A. M. *Angew. Chem., Int. Ed.* **2004**, *43*, 1419−1421.

(10) Pineda, L. W.; Jancik, V.; Roesky, H. W.; Herbst-Irmer, R. *Inorg. Chem.* **2005**, *44*, 3537−3540.

(11) Pineda, L. W.; Jancik, V.; Colunga-Valladares, J. F.; Roesky, H. W.; Hofmeister, A.; Magull, J. *Organometallics* **2006**, *25*, 2381−2383.

(12) Pineda, L. W.; Jancik, V.; Roesky, H. W.; Herbst-Irmer, R. *Angew. Chem., Int. Ed.* **2004**, *43*, 5534−5536.

(13) Pineda, L. W.; Jancik, V.; Oswald, R. B.; Roesky, H. W. *Organometallics* **2006**, *25*, 2384−2387.

(14) Jana, A.; Ghoshal, D.; Roesky, H. W.; Objartel, I.; Schwab, G.; Stalke, D. *J. Am. Chem. Soc.* **2009**, *131*, 1288−1293.

(15) Jana, A.; Nekoueishahraki, B.; Roesky, H. W.; Schulzke, C. *Organometallics* **2009**, *28*, 3763−3766.

(16) Maksic, Z. B.; Kovacevic, B. *J. Chem. Soc., Perkin Trans. 2* **1999**, 2623−2629.

(17) Arii, H.; Nakadate, F.; Mochida, K. *Organometallics* **2009**, *28*, 4909−4911.

(18) York, J. T.; Young, V. G.; Tolman, W. B. *Inorg. Chem.* **2006**, *45*, 4191−4198.

(19) Leung, W. P.; So, C. W.; Chong, K. H.; Kan, K. W.; Chan, H. S.; Mak, T. C. W. *Organometallics* **2006**, *25*, 2851−2858.

(20) Healy, P. C.; Pakawatchai, C.; Raston, C. L.; Skelton, B. W.; White, A. H. *J. Chem. Soc., Dalton Trans.* **1983**, 1905−1916.

(21) Bowmaker, G. A.; Boyd, S. E.; Hanna, J. V.; Hart, R. D.; Healy, P. C.; Skelton, B. W.; White, A. H. *J. Chem. Soc., Dalton Trans.* **2002**, 2722−2730.

(22) Oakley, S. H.; Coles, M. P.; Hitchcock, P. B. *Inorg. Chem.* **2004**, *43*, 5168−5170.

(23) Allen, D. W.; Mifflin, J. P. L; Coles, S. *Chem. Commun.* **1998**, 2115−2116.

(24) Oakley, S. H.; Soria, D. B.; Coles, M. P.; Hitchcock, P. B. *Dalton Trans.* **2004**, 537−546.

(25) Soloveichik, G. L.; Eisenstein, O.; Poulton, J. T.; Streib, W. E.; Huffman, J. C.; Caulton, K. G. *Inorg. Chem.* **1992**, *31*, 3306−3312.

(26) Alemany, P.; Alvarez, S. *Inorg. Chem.* **1992**, *31*, 4266−4275.

(27) Belsky, V. K.; Ishchenko, V. M.; Bulychev, B. M.; Soloveichik, G. L. *Polyhedron* **1984**, *3*, 749−752.

(28) Hou, H. W.; Long, D. L.; Xin, X. Q.; Huang, X. X.; Kang, B. S.; Ge, P.; Ji, W.; Shi, S. *Inorg. Chem.* **1996**, *35*, 5363−5367.

(29) Ly, H. V.; Parvez, M.; Roesler, R. *Inorg. Chem.* **2006**, *45*, 345−351.

(30) Shieh, M.; Miu, C. Y.; Lee, C. J.; Chen, W. C.; Chu, Y. Y.; Chen, H. L. *Inorg. Chem.* **2008**, *47*, 11018−11031.

(31) Albano, V. G.; Busetto, L.; Cassani, M. C.; Sabatino, P.; Schmitz, A.; Zanotti, V. *J. Chem. Soc., Dalton Trans.* **1995**, 2087−2093.

(32) Pogrebnyakov, D. A.; Starikova, Z. A.; Pavlenko, N. I.; Rubailo, A. I.; Sokolenko, V. A.; Chudin, O. S.; Antonova, A. B. *Russ. Chem. B+* **2002**, *51*, 1339−1340.

(33) Hartl, H. *Angew. Chem., Int. Ed. Engl.* **1987**, *26*, 927−928.

(34) Bowmaker, G. A.; Hart, R. D.; deSilva, E. N.; Skelton, B. W.; White, A. H. *Aust. J. Chem.* **1997**, *50*, 621−626.

(35) Ding, Y. Q.; Roesky, H. W.; Noltemeyer, M.; Schmidt, H. G.; Power, P. P. *Organometallics* **2001**, *20*, 1190−1194.

(36) Sheldrick, G. M. *Acta Crystallogr., Sect. A* **2008**, *64*, 112−122.

(37) Fjeldberg, T.; Haaland, A.; Schilling, B. E. R.; Lappert, M. F.; Thorne, A. J. *J. Chem. Soc., Dalton Trans.* **1986**, 1551−1556.